Comparison of Proposed Putative Active Conformations of Myelin Basic Protein Epitope 87−99 Linear Altered Peptide Ligands by Spectroscopic and Modelling Studies: The Role of Positions 91 and 96 in T-Cell Receptor Activation

Efthimia D. Mantzourani,[†,‡] Theodore V. Tselios,*[,‡] Simona Golic Grdadolnik,[§] James A. Platts,[∥] Andrea Brancale,[⊥] George N. Deraos,[‡] John M. Matsoukas,[‡] and Thomas M. Mavromoustakos*[,†]

National Hellenic Research Foundation, Institute of Organic and Pharmaceutical Chemistry, 48 Vassileos Constantinou Avenue, 116 35, Athens, Greece, University of Patras, Department of Chemistry, 265 00, Rion, Patras, Greece, Laboratory for Molecular Modeling and NMR Spectroscopy, National Institute of Chemistry, Hajdrihova 19, SI-1001 Ljubljana, Slovenia, Department of Chemistry, Cardiff University, Post Office Box 912, CF10 3TB, Cardiff, Wales, United Kingdom, and Welsh School of Pharmacy, Cardiff University, Redwood Building, King Edward VII Avenue, CF1 3XF, Cardiff, Wales, United Kingdom.

Received January 13, 2006

This work proposes a structural motif for the inhibition of experimental autoimmune encephalomyelitis (EAE) by the linear altered peptide ligands (APLs) [Ala^{91,96}] MBP$_{87-99}$ and [Arg^{91},Ala^{96}] MBP$_{87-99}$ of myelin basic protein. Molecular dynamics was applied to reveal distinct populations of EAE antagonist [Ala^{91,96}] MBP$_{87-99}$ in solution, in agreement with NOE data. The combination of the theoretical and experimental results led to the identification of a putative active conformation. This approach is of value as no crystallographic data is available for the APL−receptor complex. TCR contact residue Phe^{89} has an altered topology in the putative bioactive conformations of both APLs with respect to the native peptide, as found via crystallography; it is no longer prominent and solvent exposed. It is proposed that the antagonistic activity of the APLs is due to their binding to MHC, preventing the binding of self-myelin epitopes, with the absence of an immunologic response as the loss of some interactions with the TCR hinders activation of T-cells.

Introduction

Multiple sclerosis (MS)[a] is an inflammatory, demyelinating disease involving the white matter of the central nervous system (CNS)[1,2] caused by aberrant responses of autoreactive T-cells that escape negative selection. T-cell receptors (TCRs) recognize self-peptide fragments bound to major histocompatibility complex II[3,4] (MHC II) molecules (in human referred to as HLA, human leukocyte antigens), resulting in T-cell activation and proliferation and the triggering of an autoimmune response. Previous studies have demonstrated that the HLA-DR2b (DRB1*1501) haplotype is present at an increased frequency in northern European caucasoid patients with MS.[5,6]

Although the antigenic components of myelin in MS have not been identified with certainty yet, MBP is believed to be the main candidate autoantigens, and MBP$_{87-99}$ is encephalitogenic in experimental autoimmune encephalomyelitis (EAE), the best studied animal model for MS.[7−10]

FTY720[11−14] has been presented lately as an emerging therapy against MS, reducing the rate of clinical relapses in more than 50% of MS patients. It inhibits immune responses by preventing the homing of helper T-cells to lesion in peripheral organs. Its precise mechanism of action is not known, but it is likely to interfere with cell adhesion molecules. Phase III studies were planned to start in 2005. Hitherto, there had been no report of a current therapy that lacks unpredicted and dangerous side effects or that can be used in long-term treatment until recently.[15−19] Therefore, much interest has been focused on antigen-specific therapies that suppress autoreactive T-cells.[20]

An efficient approach towards the therapeutic management of MS involves the use of peptide analogues of disease-associated myelin epitopes (altered peptide ligands, APLs) that are designed to bind with high affinity to disease-associated MHC molecules but do not activate disease causing T-cells; the scope is to block the formation of the trimolecular complex MHC−APL−TCR and, therefore, to interrupt the process of the disease.[21,22] Considerable work has been done in this field[20,23−25] based on studies on MBP$_{83-99}$,[26,27] but phase II clinical trials have been suspended[28,29] due to hypersensitivity reactions in a percentage of the patients.

A new strategy is to synthesize a more hydrolytically stable molecule, for example, a cyclic peptide, that retains biological activity. In previous studies based on the immunodominant human MBP epitope 87−99, two antagonist cyclic analogues of MBP$_{87-99}$ have been designed and synthesized that are as active against EAE induced by guinea pig MBP$_{72-85}$ epitope as their linear counterparts.[30,31]

Linear peptides are a good starting point for conformational studies and rational drug design. Earlier work has been focused on an investigation of the three-dimensional (3D) structure of a linear EAE antagonist APL, [Arg^{91}, Ala^{96}] MBP$_{87-99}$.[32] At least two APLs are required for a detailed and trustworthy comparison of results, though; therefore, the extended analysis of another APL was considered essential. Our goal is to derive conclusions relevant to the putative bioactive conformation of similar peptides, to identify common features that comprise a structural motif, and, therefore, to understand better the physicochemical and structural properties required for antagonistic

* Corresponding author. Tel.: 0030-210-7273869. Fax: 0030-210-7273871. E-mail: tmavro@eie.gr.
† National Hellenic Research Foundation.
‡ University of Patras.
§ National Institute of Chemistry.
∥ Department of Chemistry, Cardiff University.
⊥ Welsh School of Pharmacy, Cardiff University.

[a] Abbreviations: MS, multiple sclerosis; CNS, central nervous system; TCR, T-cell receptor; APL, altered peptide ligand; MHC, major histocompatibility complex; HLA, human leukocyte antigens; EAE, experimental autoimmune encephalomyelitis; MBP, myelin basic protein; NMR, nuclear magnetic resonance; MD, molecular dynamics.

10.1021/jm060040z CCC: $33.50
Published on Web 10/20/2006

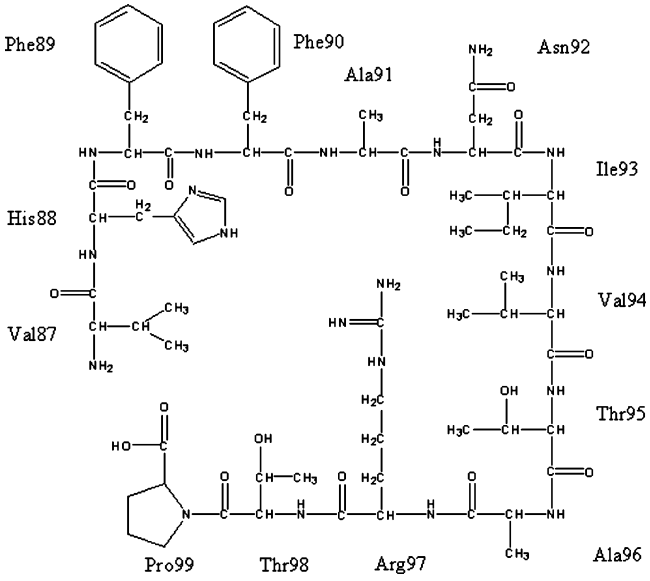

Figure 1. Structure of the linear antagonist [Ala^{91,96}] MBP$_{87-99}$.

biological activity. By the term "putative active conformation", we define the conformation that enables binding with the MHC but prevents binding with the TCR and, therefore, T-cell activation.

Within this context, the following study focuses on the conformational analysis of [Ala^{91,96}] MBP$_{87-99}$[33] (Figure 1), a rationally designed APL in which Lys^{91} and Pro^{96}, that are TCR contact sites, were substituted by Ala. A combination of experimental one-dimensional (1D) and two-dimensional (2D) NMR spectroscopic methods and restrained molecular dynamics has been applied, following the methodology established by our previous studies,[32] to reveal many energetically favored conformations and identify a possible bioactive one among them. It is known that flexible molecules are deformed when binding to proteins,[34] but it is important to use as an initial conformation for interaction with the receptor one that the molecule can actually adopt in solution and not one that only solely arises after theoretical calculations. The proposed putative bioactive conformation is indeed one of these low energy structures, in which a range of the experimental NOE distance restraints is in accordance with the conformation of MBP$_{85-99}$ provided by crystallographic data. The obtained results show that in both conformations the distance between the primary MHC anchors deviate less than 0.5 Å from the X-ray structure. The term "primary MHC anchors" refers to amino acids Val^{87} and Phe^{90}, which contact the receptor and accommodate in its pockets. The remaining residues can present different topology as long as their backbone adopts a general shape that fits in the receptor.[35]

Results and Discussion

A. Structure Identification. The proton chemical shifts of [Ala^{91,96}] MBP$_{87-99}$ in the 1D ^{1}H NMR spectrum were assigned using 2D TOCSY and NOESY experiments in combination with 2D ^{1}H-^{13}C HSQC and ^{1}H-^{13}C HSQC-TOCSY experiments (Supporting Information). Observed peaks are referenced to DMSO-d_6. For the assignment, the spin system of His^{88} was used as an initial pattern in TOCSY. Additional information was then used from the NOESY spectrum in which sequential cross-peaks occur between $C_\alpha H_i$ and NH_{i+1} resonances ($d_{\alpha N(i,i+1)}$). The cross-peak between the C_αH of Thr^{98} and the C_δH of Pro^{99} was used to establish sequential assignment. This procedure allowed the establishment of backbone sequential connectivities for the entire peptide and thus makes specific assignments for all the resonances, as summarized in Table 1.

Additionally, ^{13}C assignment was accomplished to study the conformation of the proline peptide bond. One set of resonances was observed for [Ala^{91,96}] MBP$_{87-99}$ in DMSO, demonstrating the existence of a single conformation of the Thr^{98}−Pro^{99} peptide bond. Cβ of Pro^{99} was found to be at 28.5 ppm, while Cγ was found at 24.3 ppm. The difference in ppm is 4.2, indicating that for the dominant conformers of the conformational ensemble the peptide bond of the Thr^{98} with Pro^{99} is *trans* and that *cis*−*trans* isomerization[36] does not occur. Further evidence for the *trans* nature of this peptide bond is provided by the NOE connectivities observed between α Thr^{98} with δ_1 Pro^{99} and β Thr^{98} with δ_2 Pro^{99}.

B. NOE Connectivities. The proton−proton NOE connectivities were collected from the NOESY spectrum measured at 150 ms. The list of observed inter-residue NOE connectivities is included in Supporting Information. Due to the fact that Hα Ile^{93} and Hβ Ala^{91} are totally overlapped with Hα Thr^{95} and Hγ Val^{94}, respectively, there is only a limited number of clear medium range NOE peaks.

As with most short linear peptides in solution, the molecule is expected to be fluctuating over an ensemble of conformations with their φ and ψ angles lying within the broad minima of the conformational energy[37] diagram. Indeed, observation of extended regions of both sequential NOE connectivities $d_{\alpha N(i,i+1)}$ and $d_{NN(i,i+1)}$ indicate a conformational averaging between the α_R and β regions of φ, ψ space.[38] The only deviation to this pattern comes from the middle part of the peptide, in particular the sequence Ala^{91}−Asn^{92}, where no sequential $d_{\alpha N(i,i+1)}$ NOE is observed; thus, flexibility in this part is very much reduced, and there should be a well-defined structure. The weak $d_{N\alpha(i,i+1)}$ NOE observed between the two amino acids is also unique and supports the presence of this well-determined structure.

The rest of sequential $d_{\alpha N(i,i+1)}$ are all present. Strong peaks along the entire backbone and absence of any long-range NOEs indicate the presence of a significant number of populations where [Ala^{91,96}] MBP$_{87-99}$ adopts an extended conformation. However, observation of a number of medium-range NOEs at different parts of the peptide backbone identifies the presence of populations with segments of local folded structure in the conformational ensemble.

Consecutive $d_{NN(i,i+1)}$ peaks are observed between the NH proton resonances of all but Thr^{95}−Ala^{96} and Arg^{97}−Thr^{98}, which are overlapped with the main diagonal. However, the consecutive $d_{NN(i,i+1)}$ NOE connectivities are not indicative for the presence of populations with regular helical structure, because the $d_{\alpha N(i,i+3)}$ or $d_{\alpha\beta(i,i+3)}$ connectivities that are diagnostic of a regular helix are absent.

A number of clear medium-range inter-residue NOE connectivities are observed, indicative of populations with backbone bends formed. Ile^{93} is in close proximity with Thr^{95}, as suggested by two cross-peaks between the proton resonances of Hδ−NH and NH−Hγ. There is also a population where the side chain of Thr^{95} approaches Arg^{97}, as indicated by the NOE peak between Hγ−NH.

The N−terminus presents flexibility: there are cross-peaks between Hγ Val^{87} and NH of His^{88}, as well as with the ring protons of both His^{88} and Phe^{89}. Also, there are NOE connectivities between the ring protons of His^{88} with Hβ of Phe^{89} and of Phe^{90}, as well as with NH of Phe^{89}.

C. Conformational Ensemble of [Ala^{91,96}] MBP$_{87-99}$ from the MD Trajectories. The following analysis focuses on the

Table 1. Assignment of the ^{1}H Spectrum (Top Lines in the Amino Acid Sequences), Using as a Reference DMSO Resonated at 2.49 ppm, and ^{13}C Assignment Accomplished (Bottom Lines in Amino Acid Sequences) Using a Combination of TOCSY, NOESY, ^{1}H−^{13}C HSQC, and ^{1}H−^{13}C HSQC-TOCSY Experiments and DMSO-d_6 Resonated at 39.5 ppm

amino acids	NH	α	β	γ	δ	other protons
Val87	8.06	3.59	1.97	0.82		
		56.8	29.8	17.9		
His88	8.62	4.66	β1, 2.91; β2, 2.99			2H: 7.26, 116.7
		51.0	26.9			4H: 8.93, 133.8
Phe89	8.21	4.56	β1, 2.76; β2, 2.99			ring: 7.18
		53.4	37.3			128.7, 127.7
Phe90	8.36	4.45	β1, 2.81; β2, 2.94			ring: 7.21
		53.9	37.5			129.1, 127.8
Ala91	7.95	4.19	0.84			
		57.9	17.9			
Asn92	8.2	4.6	β1, 2.36; β2, 2.53			ε1NH: 6.96
		49.4	36.7			ε2NH: 7.35
Ile93	7.71	4.21	1.7	γ1, 1.01; γ2, 1.39	0.77	γ (CH3): 0.79
		56.6	36.5	23.7	11.0	15.0
Val94	7.95	4.2	1.98	0.84		
		57.9	29.8	17.9		
Thr95	7.79	4.21	4.00	1.00		OH: 4.88
		57.9	66.1	19.2		
Ala96	7.82	4.28	1.21			
		48.1	17.9			
Arg97	7.97	4.32	β1, 1.47; β2, 1.67	1.45	3.06	εNH: 7.49
		51.3	28.8	24.5	40.2	
Thr98	7.92	4.31	3.80	1.12		OH: 4.72
		56.6	66.7	19.0		
Pro99		4.19	β1, 1.83; β2, 2.13	γ1, 1.85; γ2, 1.91	δ1, 3.63; δ2, 3.79	
		57.9	28.5	24.3	46.8	

conformations that satisfy the set of predefined criteria and comprise populations present in solution. Criteria for clustering are the following: (a) all conformers within each cluster should have backbone dihedral angles that occupy the same region of the Ramachandran map, (b) all conformers within each cluster should present a similar conformation of their side chains, and (c) root-mean-square deviation (RMSD) of all structures within a cluster should present a deviation of less than 1 Å. Eight families of conformations were identified after applying MD runs (Figure 2). The peptide parameters report for the eight families is shown in Table 2, as well as the observed and expected values of the mean and standard deviation of various measured angles.

The Ramachandran maps for all structures generated are included in Supporting Information. Out of the lowest energy conformation of each cluster (energies histogram is included in Supporting Information), family **5** is energetically favored, followed by **4**, **8**, **7**, **2**, **1**, **3**, and **6**. A key element of this conformational analysis is the barrier to conversion between different families. Figure 2 shows that families **4** and **5** differ by rotation about several backbone and side-chain dihedrals, such that isolation of an individual transition state is not feasible. Moreover, because all the structures were generated from a single MD run, rotational barriers must be of a similar order to the thermal energy kT available in the simulation (where k is Boltzmann's constant and T is the temperature, 298 K in this case). Hence, interconvention between conformations is feasible at room temperature.

C1. Backbone Dihedral Angles. All clusters have most of their backbone dihedral angles belonging in the β region of the Ramachandran map, except those of Ala^{91} that fall within the α_R region. Also, for two more amino acids, their backbone dihedrals fall within the α_R minimum: Phe^{89} in families **1**, **6**, and **8** and Ala^{96} in families **2** and **5**.

Families **5**, **6**, and **8** present an element of secondary structure in the sequence. There is a turn[39,40] in each of them, formed by the residues Thr^{95}−Thr^{98} for family **5** and residues Val^{87}−Phe^{90} for families **6** and **8**. These turns are stabilized by hydrogen bonds formed between $CO_{(i)}$−$NH_{(i+3)}$ in each case and are colored blue in the cartoon representation of the backbone in Figure 2. The strong $d_{NN(89,90)}$ and $d_{NN(96,97)}$ connectivities agree with the presence of the turns in different populations of the peptide. No other turn is identified in the final ensemble.

C2. Side Chain Flexibility. The conformation of the side chains for each amino acid of the eight different families is presented in Table 3. The chi1/chi2 angles of Ile^{93} are preserved among all structures, adopting the *trans*/*trans* conformation. Also, chi1 angles of Phe^{89}, Val^{94}, and Thr^{95} remain such that the side chains adopt gauche+ conformations for the first two and a gauche− conformation for Thr^{95} in all families. All the remaining amino acids present flexibility and adopt different combinations of conformations.

D. Consistency with NMR Data−Relative Populations. Experimentally derived distance constraints were measured in the final validated structure data (Supporting Information). They are all met by at least a threshold population in the ensemble. Thus, all selected conformations represent populations in solution, with each cluster of structures satisfying a different range of NOE distances, justifying that they are all present.

To further examine interatomic distances, histogram plots were obtained that allow the study of the distribution of values. The values in each case were bucketed, and the number of counts per bucket was plotted. Values were normalized to correct for sample size, and the results are displayed in percent. All histograms are included in Supporting Information. Percentages mentioned refer to the overall number of the selected structures. With the help of these histograms, closeness between side chains and spatial proximity of side chains with backbone was quantified (Supporting Information). Some of the NOE contacts are preserved across all clusters, though this is not the case for all. The flexibility is justified by the amount of NOE peaks present in the NOESY spectrum acquired, which could not all be satisfied in a unique conformation.

Individual populations cannot be identified by NMR solely due to their fast interconversion rate on the NMR time scale. This is a consequence of low rotational energy barrier about

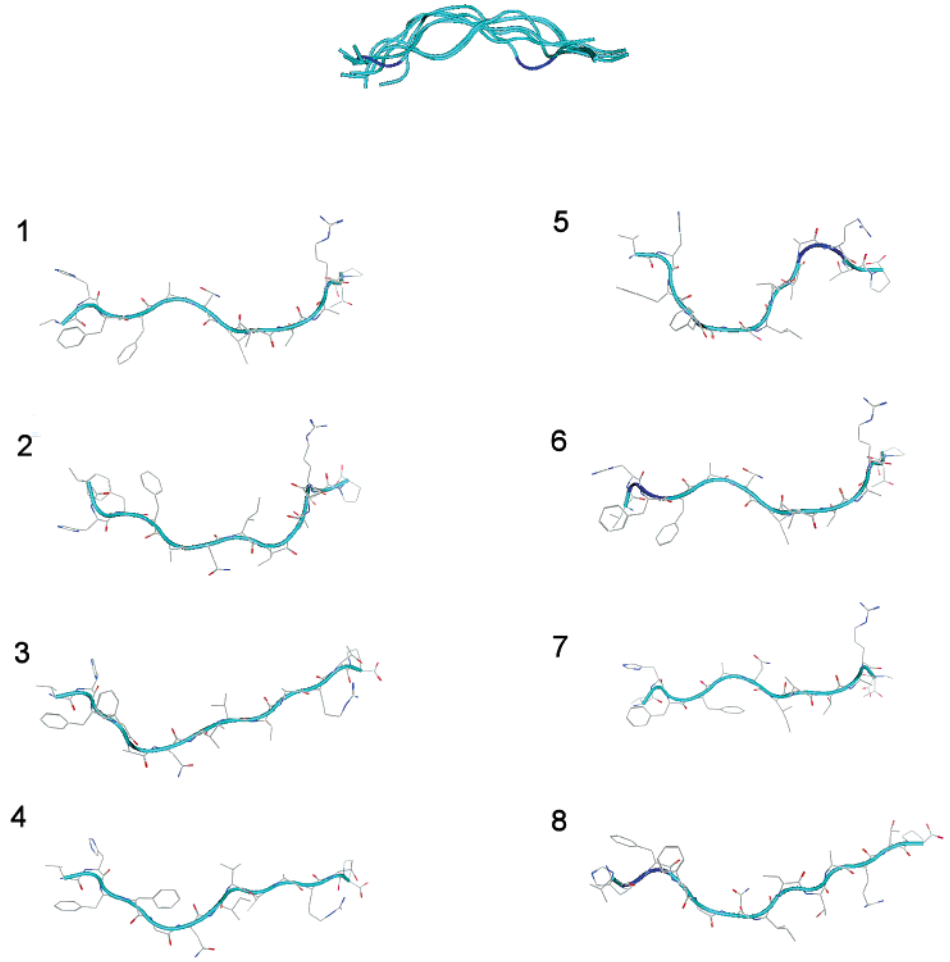

Figure 2. Lowest energy conformation of each of the eight families generated after molecular dynamics simulations, with their backbone represented as cartoon and colored blue when turns are formed.

Table 2. Peptide Parameters' Report for the 8 Families of Conformations Obtained after Molecular Dynamics Runs. Included Are the Observed and Expected Values of the Mean and Standard Deviation of Various Measured Angles

	observed		expected	
parameter	mean	s.d.	mean	s.d.
trans omega:	172.2	6.6	180	5.8
C-alpha chirality	33.9	1.3	33.8	4.2
chi1−gauche minus	−59.9	12	−66.7	15
chi1−gauche plus	50.1	14.6	64.1	15.7
chi1−*trans*	193.4	12.4	183.6	16.8
chi1−pooled s.d.		13.1		15.7
proline phi	−66.3	4.1	−65.4	11.2

the phi and psi angles in linear peptides, which is typically below 4 kcal mol^{-1}.[41] Therefore, the individual populations are spotted applying a combination of molecular dynamics and energy minimization. Theoretical methods are, therefore, a valuable supplement to NMR data for exploration of conformational space in the vicinity of conformers deduced from spectroscopic data.

E. Proposed Active Conformation of [Ala^{91,96}] MBP$_{87-99}$. Wucherpfennig et al.[35] have recently determined the structure of the trimolecular complex TCR−MBP$_{85-99}$−HLA-DR2b by crystallography using a TCR from a patient with MS. This TCR represents one of the best-characterized TCRs from a human autoimmune disease and presents a topology notably different from that of antimicrobial ones.[42−44] It contacts only the N-terminal region of the peptide rather than being centered on the peptide−MHC complex. It is believed that the aberrant binding properties increase the probability that autoreactive T-cells escape deletion in the thymus and attack self-myelin.

The 3D structure of MBP$_{85-99}$ was isolated from the complex (pdb code: 1ymm), and the segment 87−96 was used as a basis to establish criteria in order to identify a putative bioactive conformation among all the low energy conformers that were generated for the APL [Ala^{91,96}] MBP$_{87-99}$. The desired putative active conformation that we are seeking, results in optimal HLA binding affinity, with canonical MHC binding motifs. At the same time, the complex (peptide−HLA) fails to be recognized by the TCR and, therefore, there is no triggering of an immune response. It is worth mentioning that overall RMSD of the peptide with that isolated from the complex used in our previous studies (pdb code: 1bx2[45]) is only 0.515 Å. Therefore, the same set of criteria can be used, with slight changes to account for the particular behavior in the central part of the molecule. Because that part was constrained and allowed minimum flexibility throughout the MD runs, it is very likely to change once it reaches the receptor. This idea is in accordance with the general belief that peptides approach their receptor with a low-energy conformation but actually bind to it with a slightly different one,[34] caused by the changes in both protein and ligand and by the ligand's search for hydrogen bonds to the protein to replace those formed with the solvent, which are lost as the molecule enters the binding site. Therefore, the criteria set were that (a) the structure should adopt a general backbone conformation similar (C_α RMSD <1 Å) to the first six residues of the

Table 3. Conformation of Side Chains in the Eight Different Families Generated after the Molecular Dynamics Runs

	His 88 chi1/chi2	Phe 89 chi1/chi2	Phe 90 chi1/chi2	Asn 92 chi1/chi2	Ile 93 chi1/chi2	Val 94 chi1	Thr 95 chi1	Arg 97 chi1/chi2	Thr 98 chi1
1	g−/g−	g+/t	g+/g+	g−/g+	t/t	g+	g−	g+/t	t
2	g−/g−	g+/t	g+/g+	g−/g+	t/t	g+	g−	t/t	t
3	g+/g+	g+/g−	g+/t	g+/g+	t/t	g+	g−	g+/g+	g−
4	g+/t	g+/g−	t/g−	g+/g+	t/t	g+	g−	g+/g+	g−
5	g+/g+	g+/g−	g+/t	t/g+	t/t	g+	g−	g+/g+	g−
6	g−/g−	g+/t	g+/g+	g−/g+	t/t	g+	g−	g+/t	t
7	g−/g−	g+/t	t/g−	g−/g+	t/t	g+	g−	g+/t	t
8	g−/g−	g+/t	g+/g+	g−/g+	t/t	g+	g−	g+/t	t

Table 4.[a]

	MBP_{85-99}	$[Arg^{91}, Ala^{96}]$ MBP_{87-99}	$[Ala^{91,96}]$ MBP_{87-99}	RMSD (in Å)
I.				
$CB(Val^{87})$-$CB(Phe^{90})$	10.80	10.83	11.31	MBP_{85-99} – $[Arg^{91}, Ala^{96}]$ MBP_{87-99}: **0.55**
$CB(Phe^{90})$-$N(Asn^{92})$	5.72	4.90	5.37	MBP_{85-99} – $[Ala^{91,96}]$ MBP_{87-99}: **0.36**
$CB(Asn^{92})$-$CB(Ile^{93})$	5.77	6.13	5.31	$[Ala^{91,96}]$ MBP_{87-99} – $[Arg^{91}, Ala^{96}]$ MBP_{87-99}: **0.68**
$CB(Ile^{93})$-$CB(Thr^{95})$	7.56	6.71	7.83	
II.				
$CB(Val^{87})$-$CB(His^{88})$	5.95	5.70	4.99	MBP_{85-99} – $[Arg^{91}, Ala^{96}]$ MBP_{87-99}: **1.53**
$CB(Val^{87})$-ring centroid(Phe^{89})	8.74	11.07	5.58	MBP_{85-99} – $[Ala^{91,96}]$ MBP_{87-99}: **2.07**
$N(His^{88})$-ring centroid(Phe^{89})	7.27	8.69	5.02	$[Ala^{91,96}]$ MBP_{87-99} – $[Arg^{91}, Ala^{96}]$ MBP_{87-99}: **3.53**
ring centroid(Phe^{89})-N (Phe^{90})	4.83	3.50	5.89	
III.				
Dihedral chi1(Phe^{89})	69.7°	-172.1°	-58.7°	
Dihedral chi1(Phe^{90})	-164.8°	-176.3°	-168.9°	
Dihedral chi2(Phe^{90})	65.2°	57.9°	57.1	

[a] **I.** Backbone distances (in Å) between residues that serve as primary anchors for MHC binding (Val^{87}, Phe^{90}), for MBP_{85-99} obtained from the crystal structure (PDB identity 1ymm), and linear antagonists $[Arg^{91}, Arg^{96}]$ MBP_{87-99} and $[Ala^{91,96}]$ MBP_{87-99}. There has also been a comparison of backbone distances between residues that are believed to play the role of secondary MHC anchors (Asn^{92}, Ile^{93}, Thr^{95}). The column on the right shows the calculated RMSD between the molecules based on these distances. **II.** Distances between TCR contacts (His^{88}, Phe^{89}) and primary MHC anchors in the same molecules. The column on the right shows the calculated RMSD between the molecules based on these distances. **III.** Dihedral angle chi1 for Phe^{89} and dihedral angles chi1 and chi2 for Phe^{90}. The ring of Phe^{89} presents an altered topology in the two linear antagonists. In $[Ala^{91,96}]$ MBP_{87-99}, the ring of Phe^{89} approaches the backbone of the first two residues, whereas in MBP_{85-99}, its orientation is different, coming close to the backbone of Phe^{90} and being exposed for interactions with the TCR. The last proximity is also present in $[Arg^{91}, Arg^{96}]$ MBP_{87-99}, in which the N-terminus adopts a very open conformation, with the ring of Phe^{89} situated far away from Val^{87}.

natural peptide, which are important for MHC binding; (b) the C-terminal should adopt a similar general backbone conformation (C_α RMSD <1 Å) to the natural ligand; (c) the distances between amino acids that serve as primary anchors for binding to HLA-DR2b (Val^{87} and Phe^{90})[31] should have a deviation smaller than 10% compared to the X-ray structure; and (d) in conformations that fulfill criteria (a), (b), and (c), residues that are important for TCR recognition[31] (His^{88} and Phe^{89}) should be at a different position than on the natural peptide and should present different spatial relations with the residues that bind to HLA-DR2b.

All the selected conformers generated by the dynamics simulations were tested for compliance with the above criteria.

The conformation detected, to fulfill the criteria, belongs to cluster **4** and is the second lowest in energy among the lowest energy conformations of each family. In Figure 3a, it is superimposed with MBP_{87-96}, obtained from the crystal structure of the complex of MBP_{85-99} with HLA-DR2b after deleting the first two amino acids 85 and 86 for clarity. The backbones of the N-termini are almost identical. This observation may be of biological significance because it is known that the N-terminus is important for binding.[46] MHC contacts Val^{87} and Phe^{90} lie within the same region of space with respect to the natural ligand and they are available for contacts with MHC. Phe^{90} is in the correct place to approach the large hydrophobic pocket in HLA. On the other hand, TCR contact Phe^{89} has an altered topology: it is no longer prominent and solvent exposed. Therefore, it is not accessible for interaction with the TCR.

F. Comparison of the Proposed Putative Active Conformations of the APLs $[Ala^{91,96}]$ MBP_{87-99} and $[Arg^{91}, Ala^{96}]$ MBP_{87-99}: Conformational Differences and Similarities. In a previous study, we have proposed a putative bioactive conformation for $[Arg^{91}, Ala^{96}]$ MBP_{87-99}, following the procedure described above.[32] Here, we propose a putative bioactive conformation for another linear APL $[Ala^{91,96}]$ MBP_{87-99} in which the Lys^{91} and Pro^{96} residues of the native peptide

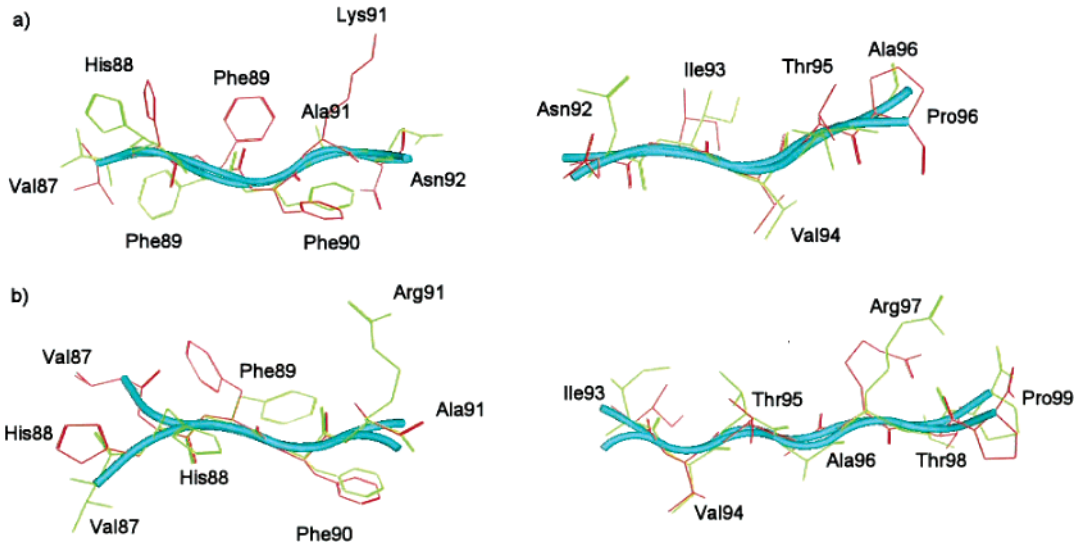

Figure 3. (a) Superimposition between MBP_{87-96} (red) obtained from the crystal structure (pdb code 1ymm) and the proposed bioactive conformation of [$Ala^{91,96}$] MBP_{87-99} (green). The backbone of all peptides is represented as a cartoon. Two different segments are used for the superimposition to show agreement with the first two criteria set for activity against MS: residues 87−91 (left−C_α RMSD: 0.74 Å) and residues 92−96 (right−C_α RMSD: 0.85 Å). The important part for binding with MHC is that primary MHC anchors (Val^{87}, Phe^{90}) occupy the same space. On the other hand, primary TCR contact Phe^{89} has a notably different orientation between the two structures. (b) Two different superimpositions between the proposed putative bioactive conformations of [Arg^{91}, Ala^{96}] MBP_{87-99} (green) and [$Ala^{91,96}$] MBP_{87-99} (red). Residues 88−90 (left−C_α RMSD is 0.21 Å) and residues 93−98 (right−C_α RMSD is 0.88 Å). Despite the difference caused by the substitution of Arg^{91} with Ala^{91}, the distance between primary MHC anchors Val^{87} and Phe^{90} differs by less than 0.5 Å: $d_{C\beta-C\beta}$ (Val^{87}−Phe^{90}) is 10.83 Å in [Arg^{91}, Ala^{96}] MBP_{87-99} and 11.31 Å in [$Ala^{91,96}$] MBP_{87-99}. The same distance is 10.80 Å in the native peptide.

MBP_{87-99} are replaced by Ala. It is important to trace the conformational similarities and differences between the two APLs because, although they differ in the position 91 of the peptide sequence, they present the same activity against MS.

Figure 3b shows two superimpositions of [Arg^{91}, Ala^{96}] MBP_{87-99} (green) and [$Ala^{91,96}$] MBP_{87-99} (red). Residues 88−91 have been overlaid (left), having C_α RMSD 0.21 Å, and residues 93−98 have been overlaid (right), having C_α RMSD 0.88 Å. Conformational changes can only be observed in the orientation of Val^{87} in the two molecules, while the rest of the N-terminus has a similar backbone conformation.

In [Arg^{91}, Ala^{96}] MBP_{87-99} there is a bulky guanidine group of Arg in position 91. Due to stereochemical hindrance, the side chain of Asn^{92} turns away and orientates itself in spatial proximity with the phenyl ring of Phe^{89}. Moreover, the imidazole group of His^{88} approaches the isopropyl group of Val^{87}. [$Ala^{91,96}$] MBP_{87-99} lacks such a bulky side chain in position 91, and the backbone has been restricted in the middle part of the molecule as a result of the experimentally derived distance constraint $d_{\alpha N(91,\,92)} > 3.5$ Å. These conformational features are responsible for the altered backbone in the N-terminus: the rings of both His^{88} and Phe^{89} come close to the side chain of Val^{87} in this case, which is situated between them.

Despite the differences described, though, it is critical to underline that in both APLs the distance between residues that are MHC anchors is similar: $d_{C\beta-C\beta}$ (Val^{87}−Phe^{90}) is 10.83 Å in [Arg^{91}, Ala^{96}] MBP_{87-99} and 11.31 Å in [$Ala^{91,96}$] MBP_{87-99}. These amino acids contact the receptor and accommodate in its hydrophobic pockets. The remaining residues can present a different topology as long as their backbone adopts a general shape that fits in the receptor.

To quantify all the mentioned similarities and differences, Kabsch's equation[47] was used, and the RMSD was calculated using the set of distances described in Table 4. The linear antagonists were compared with each other as well as with the conformation of the agonist complexed with HLA-DR2b, as found via crystallography.

The comparison of the backbone distances between the MHC primary and secondary anchors revealed very low RMSD values, affirming the similarity of the molecules regarding these residues. The native peptide [Arg^{91}, Ala^{96}] MBP_{87-99} has an RMSD value of 0.55 Å, while [$Ala^{91,96}$] MBP_{87-99} has an RMSD value of 0.36 Å. When the two APLs were compared with each other, an RMSD value of 0.68 Å was found.

Regarding the TCR contacts and the distances between the backbone of the MHC anchors with them, [Arg^{91}, Ala^{96}] MBP_{87-99} with MBP_{87-96} was found to have an RMSD value of 1.53 Å, and [$Ala^{91,96}$] MBP_{87-99} with MBP_{87-96} was found to have an RMSD value of 2.07 Å. It is interesting that, although the two APLs are similar when their MHC anchors are examined, when it comes to TCR contacts, they present a difference, with a measured RMSD value of 3.53 Å.

The combination of NMR and MD studies led to proposed bioactive conformations for both the linear synthetic APL analogues [Arg^{91}, Ala^{96}] MBP_{87-99} and [$Ala^{91,96}$] MBP_{87-99}. When superimposed to MBP_{87-99} of the complexed MBP_{85-99} obtained by crystallography, both conformations present a striking similarity in the peptide binding sequence (Val^{87}−Asn^{92}).

Conclusion

A combination of molecular dynamics calculations with NMR structure determination was followed in the present study, to generate a set of conformers that are in accordance with the most critical NOEs, representing the true flexibility of the APL [$Ala^{91,96}$] MBP_{87-99}. A unique conformation is proposed as active. This conformation has HLA-DR2b contacts occupying the same region as in MBP_{85-99}, isolated from the crystal structure with the receptor, whereas one of the two major TCR anchors has altered its orientation, preventing binding with the TCR. Interactions of the side chains that are largely populated in the conformational ensemble are present, accenting again the combination of NMR and molecular dynamics as a valuable tool for the proposal of bioactive conformations. We propose

that even when no crystallographic data is available, this approach is of value to identify a possible bioactive conformation that can be used in further studies.

The aim of this work was to correlate the linear peptides' antagonistic activity with the 3D conformation they adopt. The linear peptides [Ala^{91,96}] MBP$_{87-99}$ and [Arg^{91}, Ala^{96}] MBP$_{87-99}$ were chosen to be studied as a basis to derive useful conclusions, which will consecutively be applied to design cyclic peptides or mimetics. The detailed conformational analysis of [Arg^{91}, Ala^{96}] MBP$_{87-99}$, discussed in previous work, and [Ala^{91,96}] MBP$_{87-99}$, described in this study, led to the identification of a common structural motif, as derived from superimposition of both proposed putative active conformations. MHC anchor residues have to be in a certain spatial arrangement, with their side chains available to interact with the receptor. TCR contact Phe^{89} presents a different behavior, though; it seems that the antagonistic activity of the APLs may be due to the loss of some hydrophobic interactions with the T-cell receptor, caused by the altered topology of the phenyl side chain with respect to the native peptide as found via crystallography.

These results suggest that a thorough study of the intermolecular interactions between possible agonists and antagonists and the receptor would be useful. This knowledge of the relationship of peptide conformation and activity could then lead to the rational design and synthesis of novel peptide analogues and, ultimately, peptide mimetic molecules for the treatment of MS.

Experimental Methods

A. Synthesis of [Ala^{91,96}] MBP$_{87-99}$. Linear APL [Ala^{91,96}] MBP$_{87-99}$ was synthesized step-by-step by Fmoc/*t*-Bu methodology using 2-chlorotrityl chloride (CLTR-Cl) resin (0.7 mmol Cl−/g) and Na-Fmoc (9-fluorenylmethyloxycarboxyl)-protected amino acids, as previously described.[48] The purification and identification of peptide were achieved using reverse phase high performance liquid chromatography (RP-HPLC) and electron spray ionization (ESI) mass spectroscopy, respectively.[27]

B. Nuclear Magnetic Resonance Spectroscopy (NMR). The high-resolution NMR spectra were recorded on a Varian INOVA 600-MHz spectrometer at 298 K. Peptide in the amount of 5 mg was dissolved in 0.7 mL of DMSO-d_6.[49] The DQF-COSY,[50] ^{1}H−^{13}C HSQC,[51] and ^{1}H−^{13}C HSQC-TOCSY[51] experiments were performed with gradients. The TOCSY[52] and NOESY[53] experiments were recorded using standard pulse sequences in the phase-sensitive mode. Typically, the homonuclear proton spectra were acquired with a spectral width of 11 371 Hz, 4096 data points in t_2, 16−32 scans, 324−412 complex points in t_1, and a relaxation delay of 1−1.5 s. The mixing time in NOESY and TOCSY experiments was 150 ms and 60 ms, respectively. Heteronuclear experiments were acquired with a ^{1}H spectral width of 6936 Hz, a ^{13}C spectral width of 20 471 Hz, 1024 data points in t_2, and a relaxation delay of 1 s. The ^{1}H−^{13}C HSQC was recorded with 32 scans and 128 complex points in t_1. The ^{1}H−^{13}C HSQC-TOCSY was recorded with 128 scans, 256 complex points in t_1, and a mixing time of 32 ms.

Data were processed and analyzed with FELIX software package from Accelrys Software, Inc. Spectra were zero-filled twice and apodized with a squared sine bell function shifted by $\pi/2$ in both dimensions. Cross-peak volumes in NOESY spectra were calculated by integration routine within the FELIX software. A set of strong (up to 2.8 Å), medium (2.8−3.8 Å), and weak (3.8−5 Å) NOEs was established according to the integrated intensity of the geminal pair of protons γ_1 and γ_2 of Ile^{93}, which have a distance of 1.78 Å in all conformations.

Theoretical Calculations

A. Molecular Modeling. Computer calculations were performed on a RM 3 GHz Pentium IV workstation using MOE 2005.06 by Chemical Computing, Inc.[54] Molecular dynamics simulations were performed, employing experimental distance restraints designated by the obtained NOEs. The derived conformations represent populations of various conformers present in the NMR parameters' environment.

A1. Generating the Starting Conformation. AMBER94[55] force field was employed for all energy minimizations. An extended backbone structure of the peptide sequence was built, comprised of L-amino acids with standard parameters for all atoms.

The structure was then minimized using a succession of three methods: steepest descents (SD) algorithm to remove unfavorable steric contacts, then conjugate gradients, followed by truncated Newton (TN) to find the local minimum. The energy convergence criterion was an RMSD force ≤ 0.001 kcal mol^{-1} Å^{-1}. One distance constraint was used to comply with the experimental data: no sequential d_αN (91, 92) NOE peak was observed, implying that the peptide presents limited flexibility in this part. We estimate that the distances below 3.5 Å could be observed in the NOESY spectrum. Therefore, the lower limit for the distance constraint used was set to d_αN (91, 92) > 3.5 Å and led to a conformation that fulfills this requirement. The resulting conformation was used as initial for the molecular dynamics runs.

A2. Molecular Dynamics (MD) Studies. The MD[56−59] run was performed using AMBER94 force field. A dielectric constant of 45 was used to simulate the DMSO environment. The MD production run was performed with a time step of 0.002 ps, employing Verlet's algorithm,[60] for a duration of 1 ns. The output sampling period chosen was 2 ps. An additional length of 100 ps heating time preceded the main simulation to gradually heat the system from 1 K to the desired NMR sample solution temperature of 298 K. The number of particles in the unit cell, volume, and temperature were chosen as the thermodynamic variables that were held constant. All bond lengths involving hydrogens or lone pairs were constrained.

The experimentally derived distance d_αN (91, 92) > 3.5 Å was imported as a constraint in the MD. A weight value of 50 was chosen, which represents the proportion by which the potential energy is increased when values stray from the target distance constraint. A value of 50 was found to allow substantial deviation from the target distance to obtain a sufficient sampling, without raising significantly the total energy of the molecule.

All resulting conformations were subjected to unconstrained energy minimization to achieve the local minimum of the conformation deduced by the NMR data in each case. A direct comparison with the NMR results followed.

The structure ensemble was examined for consistencies with the distance constrain, and no violation >0.2 Å was allowed. The MD runs resulted in a number of conformations with side-chain packing that was not justified by any NOE data; therefore, an initial interatomic bump check was performed. The subensemble was then subjected to structure quality checks. Selected structures had backbone dihedral angles φ and ψ within the core region of the Ramachandran map,[61−63] and *trans* ω dihedral angles.[64] Virtual dihedral angle ζ was also examined to evaluate the planarity of C_α.

The selected low-energy structures were checked for consistency with the NOE data. The final validated structure data was grouped into eight families according to backbone and side chain dihedral angles and overall RMSD (in Å). For each cluster, an RMSD of less than 1 Å was chosen.

Acknowledgment. Present work is supported by the Ministry of Development, Secretariat of Research and Technology of Greece (Grant EPAN YB/76), as well as the Slovenian-Greek bilateral project BI-GR/02-05-007.

Supporting Information Available: Spectra, full intraresidue NOE connectivities, histogram plots of distance, and energy data from MD runs, superimpositions, and measured distances. This material is available free of charge via the Internet at http://pubs.acs.org.

References

(1) Kenealy, S. J.; Perical-Vance, M. A.; Haines, J. L. The Genetic Epidemiology of MS. *J. Neuroimmunol*. **2003**, *143*, 7−12.

(2) Prat, E.; Martin, R. The Immunopathogenesis of MS. *J. Rehabil. Res. Dev.* **2002**, *39*, 187−200.

(3) Aguado, B.; Bahram, S.; Beck, S.; Campbell, R. D.; Forbes, S. A.; Geraghty, D.; Guillaudeux, T.; Hood, L.; Horton, R.; Inoko, H.; Janer, M.; Jasoni, C.; Madan, A.; Milne, S.; Neville, M.; Oka, A.; Qin, S.; Ribas-Despuig, G.; Rogers, J.; Rowen, L.; Shiina, T.; Spies, T.; Tamiya, G.; Tashiro, H.; Trowsdale, J.; Vu, Q.; Williams, L.; Yamazaki, M. MHC Sequence Consortium. Complete Sequence and Gene Map of a Human MHC Complex. *Nature* **1999**, *401*, 921.

(4) Compston, A.; Coles, A. Multiple Sclerosis. *Lancet* **2002**, *359*, 1221.

(5) Barcellos, L.; Thomson, G. Genetic Analysis of MS in Europeans. *J. Neuroimmunol*. **2003**, *143*, 1−6.

(6) Muraro, P. A.; Vergelli, M.; Kalbus, M.; Banks, D. E.; Nagle, J.; Tranquill, L. R.; Nepom, G. T.; Biddison, W. E.; McFarland, H. F.; Martin, R. Immunodominance of a Low-Affinity Major Histocompatibility Complex-binding Myelin Basic Protein Epitope in HLA-DR4 Subjects is Associated with a Restricted T cell Receptor Repertoire. *J. Clin. Invest*. **1997**, *100*, 339−349.

(7) Zamvil, S. S.; Steinman, L. The T Lymphocyte in Experimental Allergic Encephalomyelitis. *Annu. Rev. Immunol*. **1990**, *8*, 579−621.

(8) Ota, K.; Matsui, M.; Milford, E. L.; Mackin, G. A.; Weiner, H. L.; Hafler, D. A. T-Cell Recognition of an Immunodominant Myelin Basic Protein Epitope in Multiple Sclerosis. *Nature* **1990**, *346*, 183−187.

(9) Valli, A.; Sette, A.; Kappos, L.; Oseroff, C.; Sidney, J.; Miescher. G.; Hochberger, M.; Albert, E. D.; Adorini, L. Binding of Myelin Basic Protein Peptides to Human Histocompatibility Leukocyte Antigen Class II Molecules and their Recognition by T Cells from Multiple Sclerosis Patients. *J. Clin. Invest*. **1993**, *91*, 616−628.

(10) Martin, R.; Howell, M. D.; Jaraquemada, D.; Flerlage, M.; Richert, J.; Brostoff, S.; Long, E. O.; McFarlin, D. E.; McFarland, H. F. A Myelin Basic Protein Peptide is Recognized by Cytotoxic T Cells in the Context of Four HLA-DR Types Associated with Multiple Sclerosis. *J. Exp. Med.* **1991**, *173*, 19−24.

(11) Budde, K.; Schmouder, R. L.; Brunkhorst, R.; Nashan, B.; Lucker, P. W.; Mayer, T.; Choudhury, S.; Skerjanec, A.; Kraus, G.; Neumayer, H. H. First Human Trial of FTY720, a Novel Immunodomulator, in Stable Renal Transplant Patients. *J. Am. Soc.* Nephrol. **2002**, *13*, 1073−1083.

(12) Fujino, M.; Funeshima, N.; Kitazawa, Y.; Kimura, H.; Amemiya, H.; Suzuki, S.; Li, X. K. Amelioration of Experimental Autoimmune Encephalomyelitis in Lewis Rats by FTY720 Treatment. *J. Pharmacol. Exp. Ther*. **2003**, *305*, 70−77.

(13) Gonsette, R. E. New Immunosuppressants with Potential Implication in Multiple Sclerosis. *J. Neurol. Sci*. **2004**, *223*, 87−93.

(14) Virley, D. J. Developing Therapeutics for the Treatment of Multiple Sclerosis. *J. Am. Soc.* Exp. Neurother. **2005**, *2*, 638−649.

(15) Fassas A.; Kimiskidis V. K. Stem Cell Transplantation for MS: What is The Evidence? *Blood Rev.* **2003**, *17*, 233−240.

(16) Openshaw, H.; Lund, B. T.; Kashyap, A.; Atkinson, R.; Sniecinski, I.; Weiner, L. P.; Forman, S. Peripheral Blood Stem Cell Transplantation in MS With Busulfan and Cyclophosphamide Conditioning: Report of Toxicity and Immunological Monitoring. *Biol. Blood Marrow Transplant*. **2000**, *6*, 563−575.

(17) Karp, C. L.; Biron, C. A.; Irani, D. N. Interferon β in Multiple Sclerosis: Is IL-12 Suppression the Key? *Immunol. Today* **2000**, *21*, 24−28.

(18) Coles, A. J.; Wing, M. Pulsed Monoclonal Antibody Treatment and Autoimmune Thyroid Disease in MS. *Lancet* **1999**, *354*, 1691−1695.

(19) Neuhaus, O.; Strasser-Fuchs, S.; Fazekas, F. Statins as Immunomodulators: Comparison with Interferon β in MS. *Neurology* **2002**, *59*, 990−997.

(20) Feldmann, M.; Steinman, L. Design of Effective Immunotherapy for Human Autoimmunity. *Nature* **2005**, *435*, 612−619.

(21) Vergelli, M.; Hemmer, B.; Utz, U.; Vogt, A.; Kalbus, M.; Tranquill, L.; Conlon, P.; Ling, P.; Steinman, L.; McFarland, H.; Martin, R. Differential Activation of Human Autoreactive T Cell Clones By Altered Peptide Ligands Derived from MBP_{87-99}. *Eur. J. Immunol*. **1996**, *26*, 2624−2634.

(22) Mantzourani, E. D.; Mavromoustakos, T. M.; Platts, J. A.; Matsoukas, J. M.; Tselios, T. Structural Requirements for Binding of Myelin Basic Protein (MBP) Peptides to MHC II: Effects on Immune Regulation. *Curr. Med. Chem.* **2005**, *12*, 1521−1535.

(23) Nicholson, L. B.; Murtaza, A.; Hafler, B. P.; Sette, A.; Kuchroo, V. K. A T Cell Receptor Antagonist Peptide Induces T Cells that Mediate Bystander Suppression and Prevent Autoimmune Encephalomyelitis Induced with Multiple Myelin Antigens. *Proc. Natl. Acad. Sci. U.S.A.* **1997**, *94*, 9279−9284.

(24) Brocke, S.; Gijbels, K.; Allegretta, M.; Ferber, I.; Piercy, C.; Blankensteini, T.; Martin, R.; Utz, U.; Karin, N.; Mitchell, D.; Veromaa, T.; Waisman, A.; Gaur, A.; Conlon, P.; Ling, N.; Fairchild, P. J.; Wraith, D. C.; O'Garra, A.; Fathman, G. C.; Steinman, L. Treatment of Experimental Encephalomyelitis with a Peptide Analogue of Myelin Basic Protein. *Nature* **1996**, *379*, 343−346.

(25) Smilek, D. E.; Wraith, D. C.; Hodgkinson, S.; Dwivedy, S.; Steinman, L.; McDevitt, H. O. Single Amino Acid Change in a Myelin Basic Protein Peptide Confers the Capacity to Prevent Rather than Induce Experimental Autoimmune Encephalomyelitis. *Proc. Natl. Acad. Sci. U.S.A.* **1991**, *88*, 9633−9637.

(26) Martin, R.; McFarland, H. F.; McFarlin, D. E. Immunological Aspects of Demyelinating Diseases. *Annu. Rev. Immunol*. **1992**, *10*, 153−187.

(27) Krogsgaard, M.; Wucherpfennig, K. W.; Canella, B.; Hausen, B. E.; Svejgaard, A.; Pyrdol, J.; Ditzel, H.; Raine, C.; Engberg, J.; Fugger, L. Visualization of MBP T Cell Epitopes in Multiple Sclerosis Lesions Using a Monoclonal Antibody Specific for the Human Histocompatibility Leukocyte Antigen (HLA)-DR2−MBP 85−99 Complex. *J. Exp. Med*. **2000**, *191*, 1395−1412.

(28) Bielekova, B.; Goodwin, B.; Richert, N.; Cortese, I.; Kondo, T.; Afshar, G.; Gran, B.; Eaton, J.; Antel, J.; Frank, J. A.; McFarland, H. F.; Martin R. Encephalitogenic Potential of the Myeling Basic Protein Peptide (Amino Acids 83−99) in Multiple Sclerosis: Results of a Phase II Clinical Trial with an Altered Peptide Ligand. *Nat. Am.* **2000**, *6*, 1167−1175.

(29) Kappos, L.; Comi, G.; Panitch, H.; Oger, J.; Antel, J.; Conlon, P.; Steinman, L. Induction of a Nonencephalitogenic Type 2 T Helper-Cell Autoimmune Response in MS after Administration of an APL in a Placebo-Controlled, Randomized Phase II Trial. The APL in Relapsing MS Study Group. *Nat. Am*. **2000**, *6*, 1176−1182.

(30) Matsoukas, J.; Apostolopoulos, V.; Kalbacher, H.; Papini, A. M.; Tselios, T.; Chatzantoni, K.; Biagioli, T.; Lolli, F.; Deraos, S.; Papathanassopoulos, P.; Troganis, A.; Mantzourani, E.; Mavromoustakos, T.; Mouzaki, A. Design and Synthesis of a Novel Potent Myelin Basic Protein Epitope 87−99 Cyclic Analogue: Enhanced Stability and Biological Properties of Mimics Render Them a Potentially New Class of Immunomodulators. *J. Med. Chem.* **2005**, *48*, 1470−1480.

(31) Tselios, T.; Daliani, I.; Deraos, S.; Thymianou, S.; Matsoukas, E.; Troganis, A.; Gerothanassis, I.; Mouzaki, A.; Mavromoustakos, T.; Probert, L.; Matsoukas, J. Treatment of Experimental Allergic Encephalomyelitis (EAE) by a Rationally Designed Cyclic Analogue of Myelin Basic Protein (MBP) Epitope 72−85. *Bioorg. Med. Chem. Lett.* **2000**, *10*, 2713−2717.

(32) Mantzourani, E. D.; Tselios, T. V.; Golic Grdadolnik, S.; Brancale, A.; Platts, J. A.; Matsoukas, J. M.; Mavromoustakos, T. M. A Putative Bioactive Conformation for the Altered Peptide Ligand of Myelin Basic Protein and Inhibitor of Experimental Autoimmune Encephalomyelitis [Arg^{91}, Ala^{96}] MBP_{87-99}. *J. Mol. Graphics Modell*. **2006**, *25*, 17−29.

(33) Tselios, T.; Daliani, I.; Probert, L.; Deraos, S.; Matsoukas, E.; Roy, E.; Pires, J.; Moore, G.; Matsoukas, J. Treatment of Experimental Allergic Encephalomyelitis (EAE) Induced by Myelin Basic Protein (MBP) Epitope 72−85 with Linear and Cyclic Analogues of MBP_{87-99}. *Bioorg. Med. Chem*. **2000**, *8*, 1903−1909.

(34) Nicklaus, M. C.; Wang, S.; Driscoll, J. S.; Milne, G. W. Conformational Changes of Small Molecules Binding to Proteins. *Bioorg. Med. Chem*. **1995**, *3* (4), 411−428.

(35) Hahn, M.; Nicholson, M. J.; Pyrdol, J.; Wucherpfennig, K. W. Unconventional Topology of Self-Peptide-Major Histocompatibility Complex Binding by a Human Autoimmune T Cell Receptor. *Nat. Immunol*. **2005**, *6* (5), 490−496.

(36) Fisher, G. Chemical Aspects of Peptide Bond Isomerization. *Chem. Soc. Rev*. **2000**, 119−127.

(37) Dyson, H. J.; Wright, P. E. Defining Solution Conformations of Small Linear Peptides. *Annu. Rev. Biophys. Biophys. Chem.* **1991**, *20*, 519−538.

(38) Wright, P. E.; Dyson, H. J.; Lerner, R. A. The Physical Basis for Induction of Protein-Reactive Antipeptide Antibodies. *Biochemistry* **1998**, *27*, 7167.

(39) Laskowski, R. A.; Moss, A. S.; Thornton, J. M. Main-Chain Bond Lengths and Bond Angles in Protein Structures. *J. Mol. Biol*. **1993**, *231*, 1049−1067.

(40) Morris, A. L.; McArthur, M. W.; Hutchison, E. G.; Thornton, J. M. Stereochemical Quality of Protein Structure Coordinates. *Proteins: Struct., Funct., Genet.* **1992**, *12*, 345−364.

(41) Kessler, H.; Bermel, W. *Conformational NMR in Stereochemical Analysis*; VCH Publishers: New York, 1986; Chapter 6.

(42) Garcia, K. C.; Degano, M.; Pease, L. R.; Huang, M.; Peterson, P. A.; Teyton, L.; Wilson, I. A. Structural Basis of Plasticity in T Cell Receptor Recognition of a Self-Peptide-MHC Antigen. *Science* **1998**, *279*, 1166−1172.

(43) Stewart-Jones, G. B.; McMichael, A. J.; Bell, J. I.; Stuart, D. I.; Jones, E. Y. A Structural Basis for Immunodominant Human T Cell Receptor Recognition. *Nat. Immunol*. **2003**, *4*, 657−663.
(44) Hennecke, J.; Carfi, A.; Wiley, D. C. Structure of a Covalently Stabilized Complex of a Human $\alpha\beta$ T-Cell Receptor, Influenza HA Peptide and MHC Class II Molecule, HLA-DR1. *EMBO J.* **2000**, *19*, 5611−5624.
(45) Smith, K. J.; Pyrdol, J.; Gauthier, L.; Wiley, D. C.; Wucherpfennig, K. W. Crystal Structure of HLA-DR2 (DRA*0101, DRB1*1501) Complexed with a Peptide from Human Myelin Basic Protein. *J. Exp. Med.* **1998**, *188* (8), 1511.
(46) Gerritse, K.; Deen, C.; Fasbender, M.; Ravid, R.; Boersma, W.; Claassen, E. The Involvement of Specific Antimyelin Basic Protein Antibody-Forming Cells in Multiple Sclerosis Immunopathology. *J. Neuroimmunol.* **1994**, *49*, 153.
(47) Kabsch, W. A. A Solution for the Best Rotation to Relate Two Sets of Vectors. *Acta Crystallogr., Sect. A: Found. Crystallogr.* **1976**, *32*, 922−923.
(48) Tselios, T.; Apostolopoulos, V.; Daliani, I.; Deraos, S.; Grdadolnik, S.; Mavromoustakos, T.; Melachrinou, M.; Thymianou, S.; Probert, L.; Mouzaki, A.; Matsoukas, J. Antagonistic Effects of Human Cyclic MBP_{87-99} Altered Peptide Ligands in Experimental Allergic Encephalomyelitis and Human T-Cell Proliferation. *J. Med. Chem.* **2002**, *45*, 275−283.
(49) Mavromoustakos, T.; Kolocouris, A.; Zervou, M.; Roumelioti, P.; Matsoukas, J.; Weisemann, R. An Effort To Understand the Molecular Basis of Hypertension through the Study of Conformational Analysis of Losartan and Sarmesin Using a Combination of Nuclear Magnetic Resonance Spectroscopy and Theoretical Calculations. *J. Med. Chem.* **1999**, *42*, 1714−1722.
(50) Rance, M.; Sorensen, O. W.; Bodenhausen, G.; Wagner, G.; Ernst, R. R.; Wütrich, K. Improved Spectral Resolution in COSY Proton NMR Spectra of Proteins via Double Quantum Filtering. *Biochem. Biophys. Res. Commun.* **1983**, *117*, 479−485.
(51) Willker, W.; Leibfritz, D.; Kerssebaum, R.; Bermel, W. Gradient Selection in Inverse Heteronuclear Spectroscopy. *Magn. Reson. Chem*. **1993**, *31*, 287−292.
(52) Braunschweiler, L.; Ernst, R. R. Coherence Transfer by Isotropic Mixing: Application to Proton Correlation Spectroscopy. *J. Magn. Reson*. **1983**, *53*, 521−528.
(53) Jeener, J.; Meier, B. H.; Bachmann, P.; Ernst, R. R. Investigation of Exchange Processes by Two-Dimesional NMR Spectrometry. *J. Chem. Phys*. **1979**, *71*, 4546−4553.
(54) Chemical Computing Group, Inc., 1010 Sherbrooke Street W., Suite 910, Montreal, Quebec, Canada H3A 2R7.
(55) Cornell, W. D.; Cieplak, P.; Bayly, C. I.; Gould, I. R.; Merz, K.; Ferguson, D. M.; Spellmeyer, D. C.; Fox, T.; Caldwell, J. W.; Kollman, P. A. A Second-Generation Force Field for the Simulation of Proteins, Nucleic Acids, and Organic Molecules. *J. Am. Chem. Soc*. **1995**, *117*, 5179−5197.
(56) Nikiforovich, G. V.; Vesterman, B. G.; Betins, J. Combined Use of Spectroscopic and Energy Calculation Methods for the Determination of Peptide Conformation in Solution. *J. Biophys. Chem*. **1988**, *31*, 101−106.
(57) Vesterman, B.; Saulitis, J.; Betins, J.; Liepins, E.; Nikiforovich, G. V. Dynamic Space Structure of the Leu-Enkephalin Molecule in DMSO Solution. *Biochim. Biophys. Acta* **1989**, *998*, 204.
(58) Ashish, A. G.; Kishore, R. Characterization of a Novel Type VII β-Turn Conformation for a Bioactive Tetrapeptide Rigin. *Eur. J. Biochem*. **2000**, *267*, 1455−1463.
(59) Galzitskaya, O.; Caflisch, A. Solution Conformation of Phakellistatin 8 Investigated by Molecular Dynamics Simulations. *J. Mol. Graphics Modell*. **1999**, *17*, 19−27.
(60) Verlet, L. Computer Experiments on Classical Fluids. I. Thermodynamical Properties of Lennard−Jones Molecules. *Phys. Rev*. **1967**, *159*, 98−103.
(61) Ramachandran, G. N.; Ramakrishnan, C.; Sasisekharan, V. Stereochemistry of Polypeptide Chain Configuration. *J. Mol. Biol*. **1963**, *7*, 95.
(62) Ramachandran, G. N.; Sasisekharan V. Conformations of Polypeptides and Proteins. *Adv. Protein Chem*. **1968**, *23*, 283−437.
(63) Ramakrishnan, C.; Ramachandran, G. N. Stereochemical Criteria for Polypeptide and Protein Chain Conformations—Part II Allowed Conformations for a Pair of Peptide Units. *Biophys. J.* **1965**, *5*, 909−933.
(64) Laskowski, R.; McArthur, M.; Moss, D.; Thornton, J. PROCHECK: A Program to Check the Stereochemical Quality of Protein Structures. *J. Appl. Crystallogr.* **1993**, *26*, 283−291.

JM060040Z